Sum-rule-constrained classical binary-collision model for inner-shell ionizations

C. J. Tung
Institute of Nuclear Science, National Tsing Hua University, Hsinchu, Taiwan 300, Republic of China
(Received 2 May 1980)

A model calculation of cross sections for inner-shell ionization by electrons is described. This model is based on the classical binary-collision model and modified with the application of several sum rules. It is found that the model predicts quite accurately generalized oscillator strengths and cross sections for inner-shell ionization of atoms. A comparison is made with experiment and other theoretical results.

I. INTRODUCTION

Differential and total cross sections for inner-shell ionization of atoms by electrons form part of the basic input for electron transport calculations. A formal theoretical construction of these quantities involves detailed evaluations of the wave functions of the atomic systems. This treatment is generally quite cumbersome and unrealistic for, especially, large-Z atoms.

At a more empirical level, the classical-binary-collision (CBC) model provides a simple analytic method for the calculation of atomic ionization cross sections.[1] The model has enjoyed much attention since the work of Gryzinski[2] established its relevance to the properties of atomic and molecular systems. However, it is well known that the CBC model yields poor results at threshold and very high energies.[3] In such cases there is an appreciable contribution to the cross section from the range of small momentum transfers where the CBC model is most unreliable.

In this paper, we deal with the failure of the CBC model at small momentum transfers. A scheme will be proposed to calculate generalized oscillator strengths (GOS) and hence cross sections for inner-shell ionization of atoms. Our treatment will be based on the CBC model and sum rules of exact theoretical formulations. We will apply our model to several materials and compare results with experiments and other theoretical calculations.

II. GOS FOR THE CBC MODEL

The GOS associated with the ionization of an atom from the ith shell is defined by[4,5]

$$\frac{df_i}{d\omega}=\frac{2m\omega}{k^2}\sum_{\Omega}|F_{i,\Omega}(k,\omega)|^2, \tag{1}$$

where $\hbar k$ is the momentum transfer, $\hbar\omega$ is the energy transfer, m is the electron mass, and

$$F_{i,\Omega}=\left\langle \Omega, \hbar\omega-\hbar\omega_i\left|\sum_j e^{i\vec{k}\cdot\vec{r}_j}\right|0\right\rangle. \tag{2}$$

Here $\hbar\omega_i$ is the binding energy of the ith shell and $|0\rangle$ and $|\Omega,E\rangle$ are, respectively, eigenkets of the ground state and the ionized state which is specified by its energy E and a set Ω of all the other requisite quantum numbers. The sum over $\vec{r}_j$ runs over all coordinates of electrons in the ith shell of the atom.

In the CBC model, it is convenient to define the GOS per electron as

$$\left(\frac{df}{d\omega}\right)_{\rm CBC}=\left(\frac{df_i}{d\omega}\right)\Big/N_i, \tag{3}$$

where N_i is the number of electrons per atom in the ith shell. Using a hydrogenic speed distribution of electrons in the atom, it is found that[6]

$$\left(\frac{df}{d\epsilon}\right)_{\rm CBC}=\frac{2^8}{3\pi}\frac{\epsilon\eta^3\Theta(\epsilon-\epsilon_i)}{[(\epsilon-\eta^2)^2+4\eta^2]^3}, \tag{4}$$

where $\eta=\hbar k/(2mE_{0i})^{1/2}$, $\epsilon=\hbar\omega/E_{0i}$, and $\epsilon_i=\hbar\omega_i/E_{0i}$ are dimensionless variables related to, respectively, momentum transfer $\hbar k$, energy transfer $\hbar\omega$, and binding energy $\hbar\omega_i$, E_{0i} is the mean kinetic energy of electrons in the ith shell, and Θ is the step function.

For a given (n,l) state E_{0i} is given in the Slater rule as[3]

$$E_0(n,l)=\left(\frac{Z_{\rm eff}}{n^*}\right)^2 {\rm Ry}, \tag{5}$$

where

$$\begin{aligned}Z_{\rm eff}=Z&-0.35(N_{n,l}-1)-\sum_{i=1}^{n-1}\sum_{j=0}^{i-1}N_{i,j}\\&+\delta_{l,0}\left(0.15\sum_{j=0}^{n-2}N_{n-1,j}-0.35N_{n,1}\right)\\&+0.05\delta_{n,1}\delta_{l,0}(N_{1,0}-1)\\&+\delta_{l,1}\left(0.15\sum_{j=0}^{n-2}N_{n-1,j}-0.35N_{n,0}\right),\end{aligned} \tag{6}$$

Ry is the Rydberg energy, Z is the atomic number, $N_{i,j}$ is the number of electrons in the $(n=i, l=j)$ state, $\delta_{i,j}$ is the Kronecker δ function, and $n^*=1$, 2, 3, 3.7, 4, and 4.2 corresponding to $n=1$, 2, 3, 4, 5, and 6, respectively.

The GOS of Eq. (4) suffers from an oscillator strength deficiency at small momentum transfers η. This can be seen from the μth moment of the GOS defined by

$$S(\mu)=\int \epsilon^{\mu}\left(\frac{df}{d\epsilon}\right)d\epsilon\,. \tag{7}$$

It is easy to prove that the $\mu=0$ and 1 moments of the GOS of Eq. (4) satisfy

$$S_{\mathrm{CBC}}(0)=[(a+4)\alpha+3a\beta+\gamma]/\pi \tag{8}$$

and

$$S_{\mathrm{CBC}}(1)=\{[a(\eta^2-4)+8\eta^2]\alpha+3a(\eta^2+\tfrac{4}{3})\beta + (\eta^2+\tfrac{4}{3})\gamma\}/\pi\,, \tag{9}$$

where

$$a=\eta^2-\epsilon_i\,, \tag{10}$$

$$\alpha=16\eta^3/3(a^2+4\eta^2)^2\,, \tag{11}$$

$$\beta=2\eta/3(a^2+4\eta^2)\,, \tag{12}$$

and

$$\gamma=\tfrac{1}{2}\pi-\tan^{-1}(-a/2\eta)\,. \tag{13}$$

However, in the absence of electron correlation the sum rules for the $\mu=0$ and 1 moments of the GOS are given by[7,8]

$$S(0)=1 \tag{14}$$

and

$$S(1)=\eta^2+\tfrac{4}{3}. \tag{15}$$

Figure 1 shows the results of $S_{\mathrm{CBC}}(0)$ and $S_{\mathrm{CBC}}(1)$ as a function of momentum transfer η for $\epsilon_i=0.5$ and 1. It is seen that these two moments of the GOS agree asymptotically with the sum rules, but deviate significantly from them as $\eta\ll 1$. Experiment shows that these moments should be nonzero there for optically allowed transitions.[8]

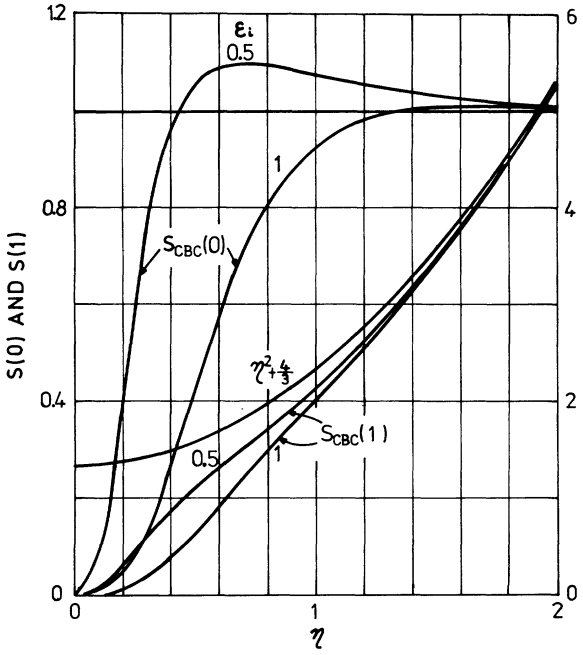

FIG. 1. The $\mu=0$ and 1 moments of the CBC model GOS as a function of momentum transfer η for $\epsilon_i=0.5$ and 1. The $\mu=0$ curves use the left ordinate scale; the $\mu=1$ curves use the right ordinate scale. The horizontal line at height 1 and the $\eta^2+\frac{4}{3}$ curve are theoretical sum-rule requirements.

III. SUM-RULE-CONSTRAINED GOS

To remedy the deficiency of the GOS of Eq. (4) at small momentum transfers, we add several terms to the numerator of the equation, viz.,

$$\frac{df}{d\epsilon}=\left(\frac{df}{d\epsilon}\right)_{\mathrm{CBC}}[A(\eta)+\epsilon B(\eta)+\epsilon^2 C(\eta)]\,. \tag{16}$$

Although we could include more terms to the expression, it seems that the present form is convenient and flexible enough for several applications. Here we will determine A, B, and C by three sum rules, namely, $S(-1)$, $S(0)$, and $S(1)$.

The sum rule for the $\mu=-1$ moment of the GOS leads to[8,9]

$$S(-1)=S_{\mathrm{inc}}(\eta)/\eta^2\,, \tag{17}$$

where $S_{\mathrm{inc}}(\eta)$ is the incoherent scattering function used in x-ray physics. For the K shell, we will use the hydrogenic result for $S(-1)$, which is given by[8]

$$S(-1)=[1-(1+\tfrac{1}{4}\eta^2)^{-4}]/\eta^2\,. \tag{18}$$

Equation (18) is expected to be unrealistic for L-shell ionization and even worse for outer shells. In these cases, we must evaluate $S(-1)$ using more realistic models, e.g., the Hartree-Slater potential model or the Hartree-Fock model.[9]

Integrating Eq. (16) and then combining it with Eqs. (14), (15), and (17), we obtain A, B, and C in terms of Eqs. (8), (9), and (19)–(21). Here

$$S_{\mathrm{CBC}}(-1)=(a\alpha+3a\beta+\gamma)/\pi\eta^2\,, \tag{19}$$

$$S_{\mathrm{CBC}}(2)=\{[a(\eta^2-12)+4(3\eta^2-4)]\alpha + [3a(\eta^2+4)+64]\beta + (\eta^2+4)\gamma\}\eta^2/\pi\,, \tag{20}$$

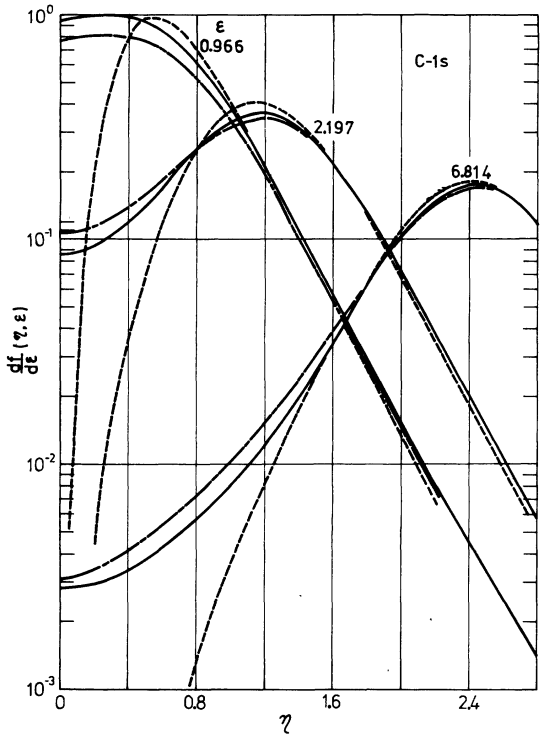

FIG. 2. Plot of GOS for carbon K-shell ionization as a function of momentum transfer η for several values of energy transfer ϵ. Solid curves are the results of present calculations; the dot-dash lines are McGuire's results of the Hartree-Slater model; the dashed curves are calculations from the CBC model of Eq. (4).

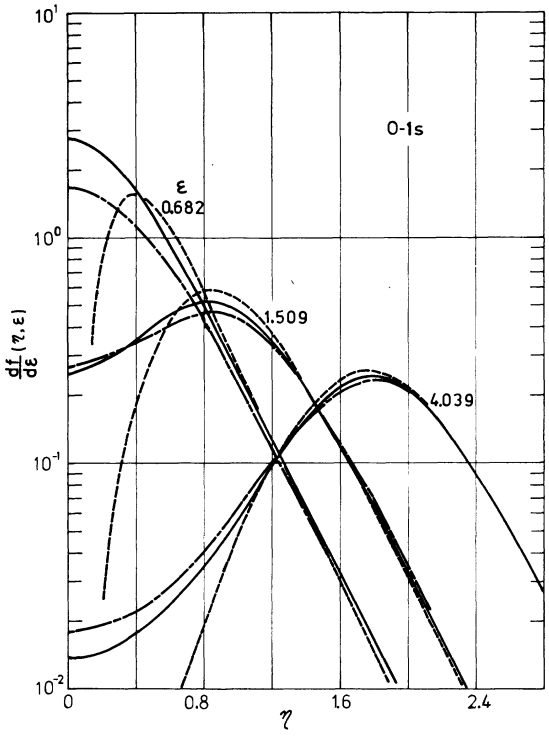

FIG. 3. Plot of GOS for oxygen K-shell ionization as a function of momentum transfer η for several values of energy transfer ϵ. Solid curves are the results of present calculations; the dot-dash lines are McGuire's results of the Hartree-Slater model; the dashed curves are calculations from the CBC model of Eq. (4).

and

$$S_{\mathrm{CBC}}(3)=\{[a(\eta^4-24\eta^2+16)+16\eta^2(\eta^2-4)]\alpha + [a(3\eta^4+24\eta^2-80)+256\eta^2]\beta + (\eta^2+4)^2\gamma\}\eta^2/\pi . \quad (21)$$

Figure 2 shows a plot of GOS for carbon K-shell ionization as a function of momentum transfer η for several values of energy transfer ϵ. A similar plot for the oxygen K shell is shown in Fig. 3. In both figures, we have plotted the numerical results of McGuire[10] which were calculated from a Hartree-Slater potential model. It is found that the present model predicts GOS for K-shell ionization quite well compared to the more detailed theoretical calculations.

Figure 4 shows the results of GOS for nitrogen L_1-shell ionization versus momentum transfer η for several values of energy transfer ϵ. Here we have calculated $S(-1)$ from McGuire's tabulations on GOS.[10] Figure 5 shows a similar plot of GOS for sodium L_1-shell ionization. The $S(-1)$ function was obtained by a fitting of Eq. (16) to the McGuire data on GOS. In both cases, our model has improved the CBC model for the GOS at small momentum transfers quite significantly. The differences between this calculation and the Hartree-Slater result are due to the uncertainty on $S(-1)$ and limited terms included in Eq. (16).

The model applies badly to the $L_{2,3}$ shell and outer shells at the region of very small momentum transfers. Again, this is due to the restriction of limited sum rules used. This restriction seems unavoidable at the present time because of the lack of data on the higher-order sum rules at the optical region.

IV. CROSS SECTIONS FOR INNER-SHELL IONIZATION BY ELECTRONS

The differential cross section for an incident electron having energy E to transfer energy $\hbar\omega$ and momentum $\hbar k$ to an atom in ionizing the ith inner shell is given in the Born approximation as[6]

$$\frac{d^2\sigma_i}{d\eta\, d\epsilon}=\frac{8\pi a_0^2 Z_2}{\xi\eta\epsilon\epsilon_{0i}^2}\frac{df}{d\epsilon}\,, \quad (22)$$

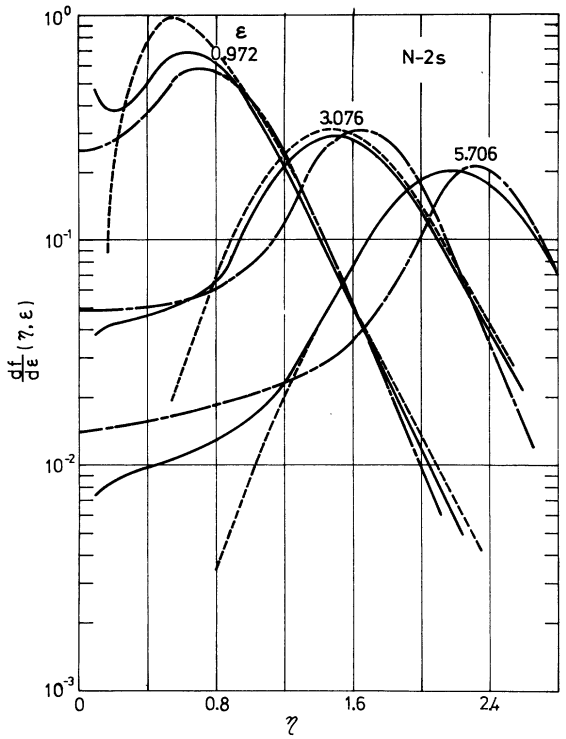

FIG. 4. Plot of GOS for nitrogen L_1-shell ionization as a function of momentum transfer η for several values of energy transfer ϵ. Solid curves are the results of present calculations; the dot-dash lines are McGuire's results of the Hartree-Slater model; the dashed curves are calculations from the CBC model of Eq. (4).

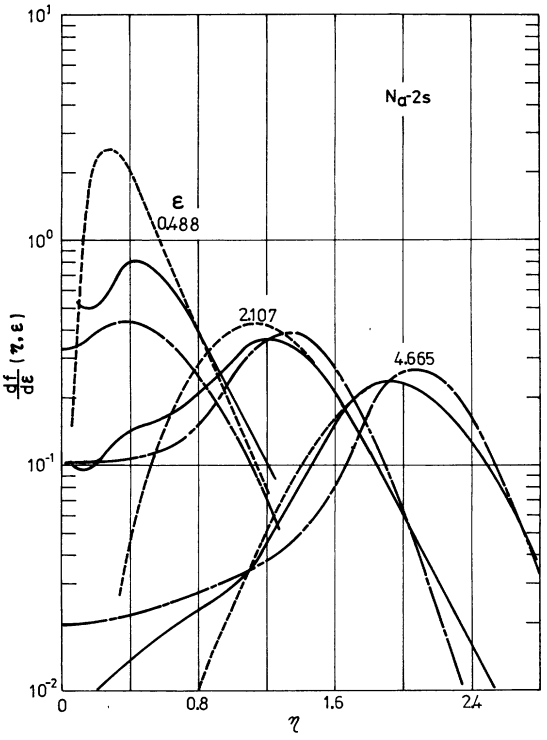

FIG. 5. Plot of GOS for sodium L_1-shell ionization as a function of momentum transfer η for several values of energy transfer ϵ. Solid curves are the results of present calculations; the dot-dash lines are McGuire's results of the Hartree-Slater model; the dashed curves are calculations from the CBC model of Eq. (4).

where a_0 is the Bohr radius, Z_2 is the number of electrons per atom in the ith shell, $\xi = E/E_{0i}$, $\epsilon_{0i} = E_{0i}/\mathrm{Ry}$, and all other variables have been defined previously. Note that the GOS in Eq. (22) is the GOS per each electron in the ith shell.

Given $d^2\sigma_i/d\eta\, d\epsilon$, the total ionization cross section for a given shell is obtained by integrating over allowed energy and momentum transfers as

$$\sigma_i = \int_{\eta_-}^{\eta_+} d\eta \int_{\epsilon_i}^{2\eta\sqrt{\xi}-\eta^2} d\epsilon \, \frac{d^2\sigma_i}{d\eta\, d\epsilon} , \tag{23}$$

where $\eta_\pm = \sqrt{\xi} \pm (\xi - \epsilon_i)^{1/2}$. The stopping power of the atom is given by

$$(\mathrm{SP})_i = E_{0i} \int_{\eta_-}^{\eta_+} d\eta \int_{\epsilon_i}^{2\eta\sqrt{\xi}-\eta^2} \epsilon \, d\epsilon \, \frac{d^2\sigma_i}{d\eta\, d\epsilon} . \tag{24}$$

Substituting Eqs. (16) and (22) into Eqs. (23) and (24), we obtain

$$\sigma_i = \frac{2^{11} a_0^2 Z_2}{3\xi\epsilon_{0i}^2} \int_{\eta_-}^{\eta_+} d\eta\, \eta^2 [A(\eta) I_0(\eta) + B(\eta) I_1(\eta) + C(\eta) I_2(\eta)] \tag{25}$$

and

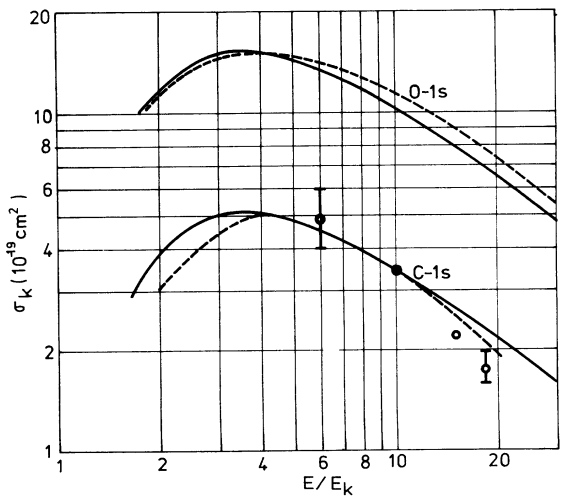

FIG. 6. Electron ionization cross sections for the K shell of C and O as a function of electron energy in units of K-shell binding energies. Solid curves are the results of present calculations. Dashed curves (Ref. 11) and experimental points (Ref. 13) are taken from Ref. 12.

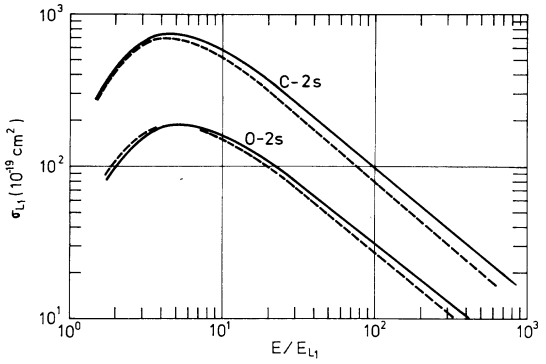

FIG. 7. Electron ionization cross sections for the L_1 shell of C and O as a function of electron energy in units of L_1-shell binding energies. Solid curves are the results of present calculations. Dashed curves are the results from numerical calculations using McGuire GOS data (Ref. 10).

$$(\mathrm{SP})_i = \frac{2^{11} a_0^2 Z_2 E_{0i}}{3\xi\epsilon_{0i}^2} \int_{\eta_-}^{\eta_+} d\eta\, \eta^2 [A(\eta) I_1(\eta) + B(\eta) I_2(\eta) + C(\eta) I_3(\eta)], \tag{26}$$

where

$$I_n(\eta) = \int_{\epsilon_i}^{2\sqrt{\xi}\,\eta - \eta^2} \frac{\epsilon^n d\epsilon}{[(\epsilon - \eta^2)^2 + 4\eta^2]^3}. \tag{27}$$

The integration in Eq. (27) may be carried out analytically.

Figure 6 shows the results of our calculations of the electron ionization cross sections for the K shell of C and O. Experimental measurements of Glupe and Mehlhorn[11] and Hink *et al.*[13] are also plotted for comparisons. Figure 7 is a plot of the electron ionization cross sections for the L_1 shell of C and O. Theoretical results from numerical calculation using McGuire GOS data[10] are also shown in the same figure.

The total stopping power of O shown in Fig. 8 is the sum of stopping powers using the present model for K and L_1 ionizations and the numerical calculations from McGuire GOS data[10] for the $L_{2,3}$ ionization. Some semiempirical results[14] along with theoretical results based on the Bethe-Block theory[15] for electron energies $E \geq 10$ keV are also plotted for comparisons.

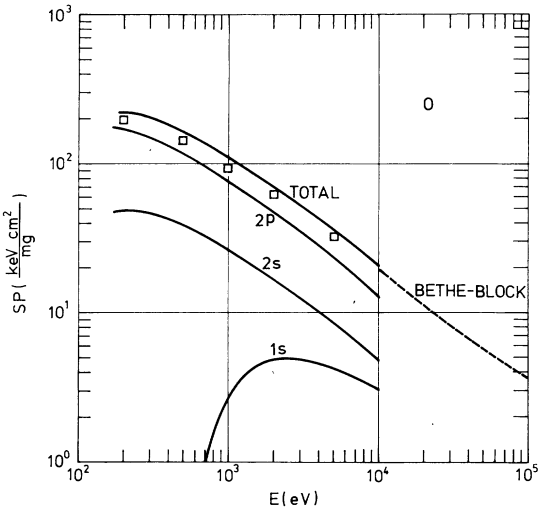

FIG. 8. Plot of stopping power of O versus electron energy. The K and L_1 results are the present calculations; the $L_{2,3}$ results are from numerical calculation using McGuire GOS data (Ref. 10). Some semiempirical results □ (Ref. 14) along with theoretical Bethe-Bloch results (Ref. 15) for electron energies $E \geq 10$ keV are taken from Ref. 16 for comparisons.

V. DISCUSSION

We have considered a model calculation of cross sections for inner-shell ionization by electrons in the nonrelativistic limit. Using scaled energy and momentum variables, we have obtained GOS and hence ionization cross sections from a procedure based on the CBC model and several selected sum rules. The model was applied using the mean kinetic energy of atomic electrons from Slater's rules.

The model has the advantage that several sum rules are satisfied automatically. As a consequence, it yields a stopping power and total cross section which reduce to the correct Bethe forms for large energies of the incident particle.[8,9] The model is capable of being applied to outer atomic shells by the addition of more terms to the GOS of Eq. (16). In such applications we will need theoretical or experimental data on the higher-order sum rules, especially near the optical region.

ACKNOWLEDGMENTS

The author expresses cordial thanks to Dr. R. H. Ritchie and Dr. J. C. Ashley for providing unpublished manuscripts and many helpful discussions. This research was supported by the National Science Council of the Republic of China.

[1]See, for example, M. R. H. Rudge, Rev. Mod. Phys. 40, 564 (1968); L. Vriens, in *Case Studies in Atomic Collision Physics* I, edited by E. W. McDaniel and M. R. C. McDowell (North-Holland, Amsterdam, 1969), p. 335.

[2]M. Gryzinski, Phys. Rev. 148, 54 (1959); 138, A305 (1965); 138, A322 (1965); 138, A336 (1965).

[3]B. B. Robinson, Phys. Rev. 140, A764 (1965).

[4]C. J. Tung and R. H. Ritchie, Phys. Rev. B 16, 4302 (1977).

[5]Strictly speaking, the GOS of an atom is not separable into contributions from each shell. Nevertheless, we expect that such separation may not lead to large errors.

[6]R. H. Ritchie, J. C. Ashley, and Dayashankar, in Rome Air Development Center Report No. RADC-TR-77-74, 1977, pp. 25–43 (unpublished).

[7]U. Fano and J. E. Turner, in National Academy of Sciences-National Research Council Report No. 1133, 1964, pp. 49–67 (unpublished).

[8]M. Inokuti, Rev. Mod. Phys. 43, 297 (1971).

[9]M. Inokuti, R. P. Saxon, and J. L. Dehmer, Int. J. Radiat. Phys. Chem. 7, 109 (1975).

[10]E. J. McGuire, Sandia Research Report No. SC-RR-70-406 (unpublished); Phys. Rev. A 3, 267 (1971).

[11]G. Glupe and W. Mehlhorn, Phys. Lett. 25A, 274 (1967).

[12]V. M. Pessa and W. R. Newell, Phys. Scr. 3, 165 (1971).

[13]W. Hink and A. Z. Ziegler, Z. Phys. 226, 222 (1969).

[14]L. R. Peterson and A. E. S. Green, Proc. Phys. Soc. London 2, 1131 (1968).

[15]L. Pages, E. Bertel, H. Joffre, and L. Skavenitis, At. Data 4, 1 (1972).

[16]H. Sugiyama, Jpn. J. Appl. Phys. 15, 1779 (1976).